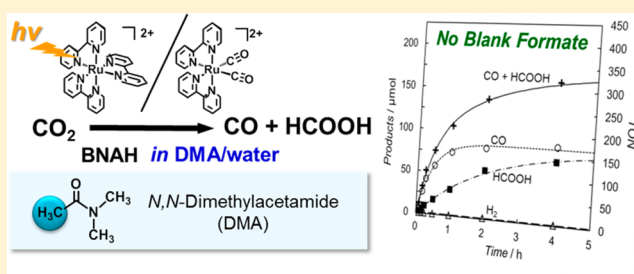


Photocatalytic CO₂ Reduction in *N,N*-Dimethylacetamide/Water as an Alternative Solvent SystemYusuke Kuramochi,[†] Masaya Kamiya,[†] and Hitoshi Ishida^{*,†,‡}[†]Department of Chemistry, Graduate School of Science, Kitasato University, 1-15-1 Kitasato, Minami-ku, Sagami-hara, Kanagawa 252-0373, Japan[‡]Precursory Research for Embryonic Science (PRESTO), Japan Science and Technology Agency (JST), 4-1-8 Honcho, Kawaguchi, Saitama 332-0012, Japan

Supporting Information

ABSTRACT: *N,N*-Dimethylacetamide (DMA) was used for the first time as the reaction solvent in the photocatalytic reduction of CO₂. DMA is highly stable against hydrolysis and does not produce formate even if it is hydrolyzed. We report the catalytic activities of [Ru(bpy)₂(CO)₂](PF₆)₂ (bpy = 2,2'-bipyridine) in the presence of [Ru(bpy)₃](PF₆)₂ as a photosensitizer and 1-benzyl-1,4-dihydronicotinamide (BNAH) as an electron donor in DMA/water. In the photochemical CO₂ reduction, carbon monoxide (CO) and formate are catalytically produced, while dihydrogen (H₂) from the reduction of water is scarcely evolved. We verified that BNAH is oxidized to afford BNA dimers during the photocatalyses in DMA/water. The plots of the production for the CO₂ reduction versus the water content in DMA/water show that the 10 vol % water content gives the highest amount of the reduction products, whose reaction quantum yields (Φ') are determined to be 11.6% and 3.2% for CO and formate, respectively. The results are compared with those in the *N,N*-dimethylformamide (DMF)/water system, which has been typically used as the solvent system for the CO₂ reduction.



INTRODUCTION

Metal complexes can be designed on the molecular levels, enabling us to provide highly active catalysts. The photocatalytic CO₂ reduction using metal complexes has attracted much attention toward construction of artificial photosynthetic systems and solar fuels.¹ In most cases of catalytic CO₂ reduction by metal complexes, the reduction products are carbon monoxide (CO) and/or formate (HCOO⁻). While the artificial photosynthetic systems have recently been developed by combining semiconductors with ruthenium bipyridyl carbonyl complexes such as [Ru(bpy)₂(CO)₂]²⁺, *trans*-(Cl)-Ru(bpy)(CO)₂Cl₂, and the derivatives as the CO₂ reduction catalysts,² the evaluations of the catalytic activities of the metal complexes toward CO₂ reduction are still carried out in organic homogeneous solution.³

N,N-Dimethylformamide (DMF) has been well-used as the reaction solvent for the CO₂ reduction due to the high solubilities of CO₂ and the metal complexes.^{3–5} However, Vos et al. have recently pointed out a problem; namely, that DMF readily hydrolyzes to give formate in the presence of water and amine, making it difficult to quantify formate for the CO₂ reduction.⁶ They have also indicated that hydrolysis of DMF would occur not during CO₂ reduction but in the course of an analytical process such as ion exchange chromatographic analysis, which usually requires the addition of water to quantify formate. As long as DMF is used as the solvent for

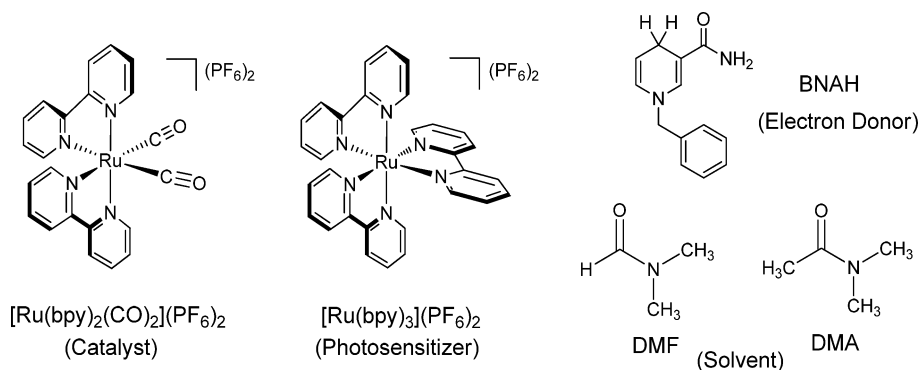
CO₂ reduction, a careful calibration is required to quantify formate produced in CO₂ reduction.

In this Report, we propose *N,N*-dimethylacetamide (DMA) as an alternative solvent for the photocatalytic CO₂ reduction. To evaluate the effectiveness of this solvent, we selected the photocatalytic system consisting of [Ru(bpy)₂(CO)₂](PF₆)₂ (bpy = 2,2'-bipyridine) as the catalyst, [Ru(bpy)₃](PF₆)₂ as the photosensitizer, and 1-benzyl-1,4-dihydronicotinamide (BNAH) as the electron donor (Chart 1). The photocatalytic system, which was originally reported by Ishida and Tanaka et al., has yielded both CO and formate as the CO₂ reduction products in DMF/water in the absence of amines such as triethanolamine or triethylamine.⁵ The selectivity for CO/formate in the CO₂ reduction has been elucidated by the equilibrium reactions among the carbonyl complex ([Ru(bpy)₂(CO)₂]²⁺), the carboxylic acid complex ([Ru(bpy)₂(CO)(C(O)OH)]⁺), and the η¹-CO₂ adduct ([Ru(bpy)₂(CO)(CO₂)]).⁷ In the catalysis, water acts as the proton source to accept the oxide anion from the coordinated CO₂ to produce CO and OH⁻. This is in contrast to the catalytic systems consisting of the rhenium complexes, which selectively produce CO with CO₃²⁻ by the oxide-transfer reaction between two CO₂ molecules.^{3d,e,8} The catalytic CO₂ reduction systems using DMF/water as the solvent should be reevaluated

Received: October 4, 2013

Published: March 14, 2014

Chart 1. Structures of the Ruthenium(II) Complexes, the Electron Donor, and the Solvents



particularly for formate production. We then examine the photocatalyses in DMA/water, and the results are compared to the ones in DMF/water. We also investigate the oxidation products of BNAH and the effect of the water contents in the DMA/water on the photocatalytic CO_2 reduction.

EXPERIMENTAL SECTION

Materials. The ruthenium complexes $[\text{Ru}(\text{bpy})_2(\text{CO})_2](\text{PF}_6)_2$ and $[\text{Ru}(\text{bpy})_3](\text{PF}_6)_2$ were prepared according to the literature.⁹ BNAH and the oxidized dimer products (4,4'-BNA₂ and two diastereoisomers of 4,6'-BNA₂) were prepared according to the literature¹⁰ and stored in a refrigerator. DMA (Wako, dehydrate), DMF (Watanabe Chemical, special grade), DMA-*d*₉ (Cambridge Isotope Lab.), DMF-*d*₇ (TCI), and Ba¹³CO₃ (Cambridge Isotope Lab.) were used as supplied. No residual triethylamine was observed in the solvents on the NMR analyses. High-purity water (resistivity: 18.2 MΩ cm) was obtained by an ultrapure water system (RFU424TA, Advantec).

Photocatalytic CO₂ Reduction. Ar-saturated DMA/water or DMF/water solutions (5 mL) of $[\text{Ru}(\text{bpy})_2(\text{CO})_2](\text{PF}_6)_2$ (1.0×10^{-4} M), $[\text{Ru}(\text{bpy})_3](\text{PF}_6)_2$ (5.0×10^{-4} M), and BNAH (0.10 M) were placed in quartz tubes (23 mL volume, i.d. = 14 mm). Each solution was bubbled through a septum cap with CO₂ gas for 20 min. Ten tubes were set in a merry-go-round irradiation apparatus (Riko Kagaku, RH400–10W) and then were irradiated using a 400 W high-pressure mercury lamp at $\lambda > 400$ nm (Riko Kagaku, L-39 cutoff filter). The reaction temperature was maintained at 298 ± 3 K by using a water bath. After they were irradiated for a definite time, the gaseous phase was analyzed for CO and H₂ content on a gas chromatography (GC) system based on a Shimadzu GC-2014. The product gases (0.10 mL) were injected with a gastight syringe into the GC equipped with successive Porapak-N, Molecular Sieve 13X, and Shimalite-Q columns (stainless steel columns). N₂ (>99.9995%) was used as the carrier gas. CO was methanized through a Shimadzu MTN-1 methanizer, followed by detection with flame ionization detector (FID). H₂ was detected with thermal conductivity detector (TCD). Formate was extracted as formic acid with ethyl acetate prior to the GC analyses as follows.¹¹ A portion of the resulting solution (2 mL) was placed in a sample tube. After adding water to adjust the water content to 50 vol %, 1.0 M sulfuric acid was added (10 vol % of the resulting DMA/water solution). The same amount of ethyl acetate as that of the acidified resulting solution was added, and the mixed solution was shaken for 10 s and stood for 2 min to extract formic acid. The upper phase (2 μL) was injected into a Shimadzu GC-2014 equipped with DB-WAX columns (i.d. 0.53 mm, 15 m \times 2). Formic acid was detected with FID after methanization by a Shimadzu MTN-1 methanizer. The reliability of quantification of formate on the GC was confirmed by the fact that the results matched with the ones using an Otsuka Electrons CAPI-3300I capillary electrophoresis analyzer within experimental errors. Time dependence of the reaction was pursued by analyzing each reaction tube with different irradiation times.

¹³C NMR Study for Photocatalytic CO₂ Reduction. The DMA-*d*₉/water (9:1 v/v, 0.83 mL) or DMF-*d*₇/water (9:1 v/v, 0.83 mL)

solution containing $[\text{Ru}(\text{bpy})_2(\text{CO})_2](\text{PF}_6)_2$ (1.0×10^{-4} M), $[\text{Ru}(\text{bpy})_3](\text{PF}_6)_2$ (5.0×10^{-4} M), and BNAH (0.10 M) in an NMR tube (i.d. = 4 mm) was bubbled with ¹³CO₂ gas, which was generated by addition of 1.0 M sulfuric acid to Ba¹³CO₃ powder. After photoirradiation using a 400 W high-pressure mercury lamp ($\lambda > 400$ nm; Riko Kagaku, L-39 cutoff filter) in a merry-go-round irradiation apparatus (Riko Kagaku, RH400–10W) for 3 h, the ¹³C NMR spectra were measured on a Bruker AVANCE II 600 spectrometer.

Quantum Yield Determination. The quantum yields of the photochemical CO₂ reduction were determined using K₃[Fe(C₂O₄)₃] as the chemical actinometer.¹² The definition of the quantum yields for the photochemical CO₂ reduction is discussed in this Report. The experimental procedure using the chemical actinometer is the following: the DMA/water (9:1 v/v, 4 mL) solution containing $[\text{Ru}(\text{bpy})_2(\text{CO})_2](\text{PF}_6)_2$ (1.0×10^{-4} M), $[\text{Ru}(\text{bpy})_3](\text{PF}_6)_2$ (5.0×10^{-4} M), and BNAH (0.10 M) in a square quartz cuvette (1.0 cm) was bubbled with CO₂ gas for 30 min and was irradiated with a 500 W superhigh-pressure mercury lamp (Ushio, USH-500D) through a Toshiba Y-43 glass filter ($\lambda > 400$ nm) for 5, 10, and 15 min. The rate of the photochemical CO₂ reduction was determined by amounts of CO and formate. The photochemical generation of Fe(II) ion from K₃[Fe(C₂O₄)₃] was quantified by reacting with 1,10-phenanthroline, followed by measuring the absorption spectra on a Shimadzu MultiSpec-1500 spectrometer. The quantum yields were also determined with a Shimadzu absolute photoreaction quantum yields measurement system QYM-01 equipped with a 460 nm band-pass filter and a 300 W Xe lamp and were confirmed to be the same results as the values obtained using the aforementioned chemical actinometer.

HPLC Analyses for Oxidation Products of BNAH. To pursue the oxidation products of the electron donor, BNAH, the reaction solutions were analyzed with high performance liquid chromatography (HPLC). Analyses were performed on a Shimadzu LC-10Ai system equipped with a Tosoh TSKgel ODS-80Ts column (4.6 mm i.d. \times 15 cm). A CH₃OH/water (55:45 v/v) solution was used as an eluent with flow rate of 1.0 mL/min (column temperature: 313 K), and a Shimadzu SPD-M20A prominence diode array was used as the detector. The retention times under the analytical conditions were determined using the authentic samples: BNAH 9.6 min, 4,6'-BNA₂ 7.0 and 9.6 min, 4,4'-BNA₂ 15.7 min, and BNA⁺ 3.4 min.

Quenching Experiments. Emission from the excited states of $[\text{Ru}(\text{bpy})_3](\text{PF}_6)_2$ in the Ar-saturated DMA/water solutions were recorded on a Hitachi F-4500 spectrometer ($\lambda_{\text{ex}} = 453$ nm) in the absence and presence of the quencher BNAH or BNA₂. The Stern–Volmer relationship (eq 1) was obtained by the plots of the relative emission intensity (I_0/I) versus the concentration of the quencher ($Q = \text{BNAH}$ or BNA_2):

$$I_0/I = 1 + K_{\text{SV}}[Q] = 1 + k_q\tau[Q] \quad (1)$$

where I_0 and I represent the intensity at 620 nm in the absence and the presence of the quencher, respectively, and K_{SV} , k_q , and τ are the Stern–Volmer constant, the quenching rate constant, and the emission lifetime, respectively. The emission lifetimes were measured at 298 K

with a FluoroCube fluorescence lifetime spectrometer (Horiba Jobin Yvon) using a 455 nm laser diode (NanoLED).

Electrochemical Measurements. Cyclic voltammograms (CV) and differential pulse voltammograms (DPV) were obtained by a Bio-Logic VSP potentiostat using an EC-Lab software. Measurements were conducted in DMA/water containing tetrabutylammonium perchlorate (${}^n\text{Bu}_4\text{NClO}_4$, 0.10 M) as a supporting electrolyte under Ar using a BAS microcell. As the electrodes, a BAS glassy-carbon working electrode, a BAS Pt counter electrode, and a BAS RE-7 reference electrode (Ag/AgNO_3 , 0.01 M in acetonitrile) were used.

RESULTS AND DISCUSSION

Photocatalytic CO_2 Reduction in DMF/Water. Photocatalytic CO_2 reduction has been carried out by photoirradiating ($\lambda > 400$ nm) the CO_2 -saturated DMF/water (9:1, v/v) solution containing $[\text{Ru}(\text{bpy})_2(\text{CO})_2]^{2+}$ (1.0×10^{-4} M), $[\text{Ru}(\text{bpy})_3]^{2+}$ (5.0×10^{-4} M), and BNAH (0.10 M), which act as the catalyst, the photosensitizer, and the sacrificial electron donor, respectively. In general, the amines (e.g., triethanolamine and triethylamine) or ascorbate has been utilized as the electron donor for photochemical H_2 evolution. One reason why we have chosen BNAH is that the amines are known not to work as the electron donor in aqueous solution, in which amines are protonated and lose the electron-donating abilities.^{5a} On the other hand, we have carried out the photocatalytic CO_2 reductions using sodium ascorbate (0.10 M) instead of BNAH as the electron donor in DMF/water (1:1, v/v) containing $[\text{Ru}(\text{bpy})_2(\text{CO})_2](\text{PF}_6)_2$ (1.0×10^{-4} M) and $[\text{Ru}(\text{bpy})_3](\text{PF}_6)_2$ (5.0×10^{-4} M); however, no reduction product of CO_2 was obtained. This is another reason why we have selected BNAH. In this Report, we have irradiated with visible light (>400 nm) for all the photocatalytic reactions because neither $[\text{Ru}(\text{bpy})_2(\text{CO})_2]^{2+}$ nor BNAH has any appreciable absorption above 400 nm. In this condition, the photosensitizer $[\text{Ru}(\text{bpy})_3]^{2+}$ was selectively excited by the photoirradiation.

The time courses of the photochemical reduction in a CO_2 -saturated and Ar-saturated DMF/water (9:1, v/v) solution are shown in Figure 1a,b, respectively. The gaseous products (CO and H_2) are analyzed with GC, and formate is also quantified with GC by acidifying it to formic acid. Thus, we denote "HCOOH" in the figures as analyzed by GC, although the word "formate" is used in the text. The ^{13}C NMR experiment in DMF- d_7 /water (9:1 v/v) using $^{13}\text{CO}_2$ indicates that CO and formate originate from CO_2 (see Supporting Information, Figure S1); however, 25 μmol of formate is detected in the photoreaction under Ar atmosphere (Figure 1b). It suggests that the hydrolysis of DMF partly occurs. Time-independent detection of formate strongly suggests that the decomposition of DMF occurs not during the photoirradiation but during the GC analyses. Actually, the capillary electrophoresis analyses scarcely detected formate in the Ar-saturated photoreaction solution. Figure 1a shows production of approximately 110 μmol (TON ≈ 220) of formate and 55 μmol (TON 110) of CO at 2 h, but we estimate the formate production by CO_2 reduction at 85 μmol (TON 170) by taking account of the production (25 μmol) from hydrolysis of DMF. Figure 1b shows that catalytic evolution of dihydrogen (H_2 ; 43 μmol , TON 85) occurs by the reduction of water in Ar-saturated solution. On the other hand, H_2 scarcely evolves in CO_2 -saturated solution (Figure 1a), indicating that the catalyst selectively reduces CO_2 .

Photocatalytic CO_2 Reduction in DMA/Water. It has been considered that changing the solvent system would be a

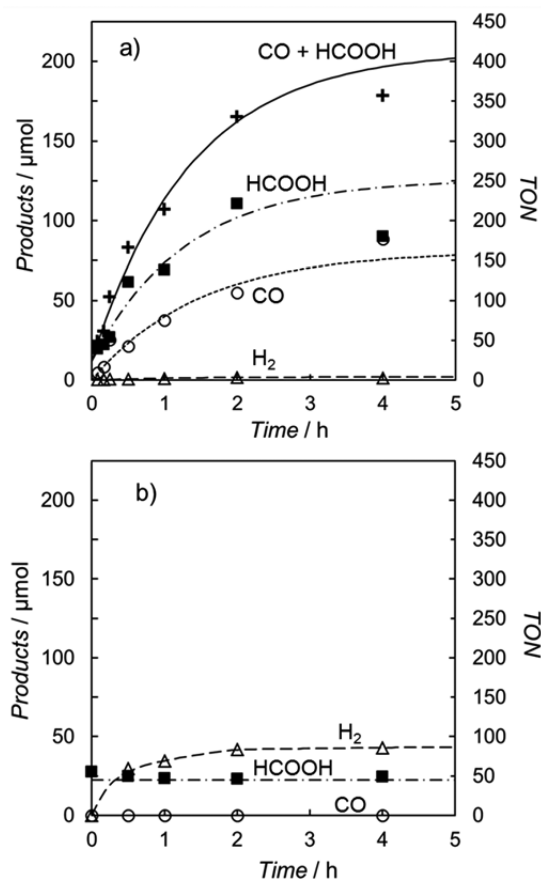


Figure 1. Photoirradiation time dependence of products in the (a) CO_2 and (b) Ar-saturated DMF/water (9:1, v/v) solution containing $[\text{Ru}(\text{bpy})_2(\text{CO})_2](\text{PF}_6)_2$ (1.0×10^{-4} M), $[\text{Ru}(\text{bpy})_3](\text{PF}_6)_2$ (5.0×10^{-4} M), and BNAH (0.10 M): CO (○), HCOOH (■), H_2 (△), and $\text{CO}+\text{HCOOH}$ (+).

simple solution to avoid the formate production from DMF hydrolysis. To search for the alternative solvent, we initially examined the photocatalytic CO_2 reduction in some common solvents such as acetone, ethanol, and acetonitrile instead of DMF (Supporting Information, Figure S2). However, the catalytic activities are dramatically depressed in such solvent systems. In the solvent systems we have examined, DMA gives a good result. DMA has higher resistance to hydrolysis than DMF, and DMA does not afford formate but acetate even if it is hydrolyzed.¹³ Figure 2a,b shows the time courses of the photoreaction in CO_2 and Ar-saturated DMA/water (9:1, v/v), respectively. Figure 2b shows no formate yield in the absence of CO_2 , indicating that the use of DMA enables us to quantify formate with GC, which requires heat. Figure 2a shows that 56 μmol (TON 112) of formate and 82 μmol (TON 164) of CO at 2 h.

We carried out the photoreduction in the $^{13}\text{CO}_2$ -saturated DMA- d_9 /water (9:1, v/v) solution and confirmed that CO and formate come from CO_2 (Figure 3). As also observed in DMF- d_7 /water, no other ^{13}C peaks including $\text{H}^{13}\text{CO}_3^-$ or $^{13}\text{CO}_3^{2-}$ originating from the $^{13}\text{CO}_2$ reduction are found. This result supports the idea that the catalytic reaction by $[\text{Ru}(\text{bpy})_2(\text{CO})_2]^{2+}$ proceeds not via the oxide-transfer between two CO_2 molecules but by the proton-coupled electron transfer.^{3d,e,7} The NMR spectra of the resulting DMA/water solution did not show any signals of acetic acid, indicating that the decomposition of DMA did not occur during the photo-

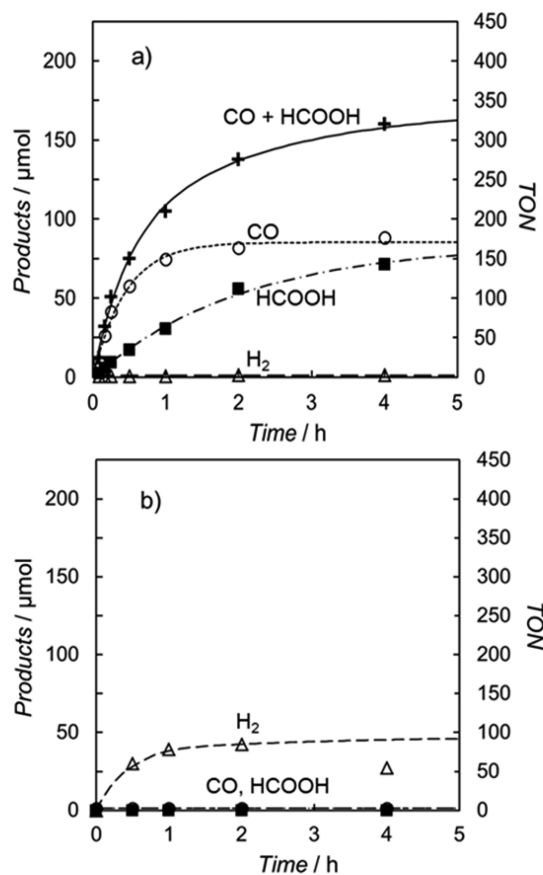


Figure 2. Photoirradiation time dependence of products in the (a) CO_2 and (b) Ar-saturated DMA/water (9:1, v/v) solution containing $[\text{Ru}(\text{bpy})_2(\text{CO})_2](\text{PF}_6)_2$ (1.0×10^{-4} M), $[\text{Ru}(\text{bpy})_3](\text{PF}_6)_2$ (5.0×10^{-4} M), and BNAH (0.10 M): CO (○), HCOOH (■), H_2 (Δ), and CO+HCOOH (+).

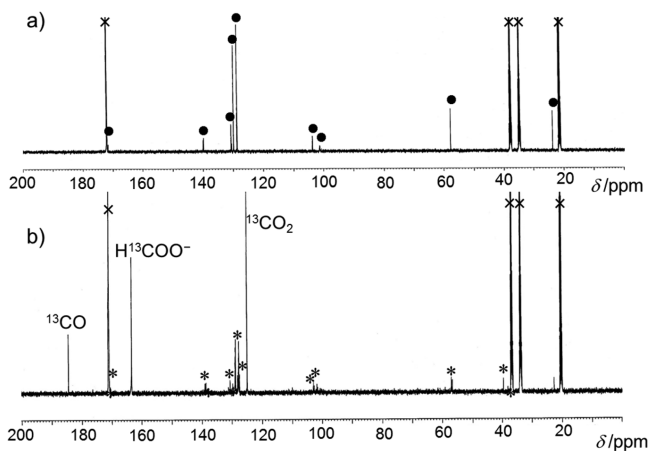


Figure 3. The ^{13}C NMR spectra of DMA- d_9 /water (9:1, v/v) solution containing $[\text{Ru}(\text{bpy})_2(\text{CO})_2](\text{PF}_6)_2$ (1.0×10^{-4} M), $[\text{Ru}(\text{bpy})_3](\text{PF}_6)_2$ (5.0×10^{-4} M), and BNAH (0.10 M) (a) before and (b) after bubbling with $^{13}\text{CO}_2$ gas followed by photoirradiation ($\lambda > 400$ nm) for 3 h. The peaks marked with (x), (●), and (*) are assigned to DMFA, BNAH, and BNA dimers,¹⁴ respectively.

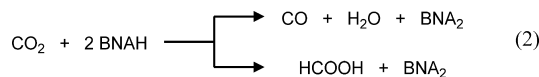
chemical reaction. The peaks for BNAH in the ^{13}C NMR spectrum decrease after the photoirradiation. With decreasing peaks for BNAH, the new peaks appear, which are not assigned to BNA^+ but to BNA dimers. This suggests that BNA dimers form as the oxidation products of BNAH. The identification

and quantification of the BNA dimers will be described in the next section.

The initial reaction rate for the CO_2 reduction, namely, the production rates for the sum of CO and formate in DMA/water, is comparable to that in DMF/water (see Figures 1a and 2a). However, the rate in the DMA/water system seems to become slow after 1 h of photoirradiation. This is because the result in DMF/water contains the formate production by the hydrolysis of DMF. If the amounts of formate produced under Ar are subtracted from the total ones, the results become quite comparable to the results in DMA/water.

Although the catalytic activities in DMF/water after the correction are similar to those in DMA/water, the selectivities for formate/CO are different. In DMA/water, CO rather than formate evolves (see Figure 2a). On the other hand, the amounts of formate in DMF/water before the correction look larger than those of CO (Figure 1a), but after the correction the amounts of formate become quite similar to those of CO. The selectivity for formate/CO has been explained by the equilibrium reactions among the carbonyl, the carboxylic acid, and $\eta^1\text{-CO}_2$ complexes: the use of strong acids with low $\text{p}K_a$ gives CO, while weak acids with high $\text{p}K_a$ provide formate.⁷ The results might be elucidated by assuming that H_2O acts as the stronger acid in DMA than it does in DMF. Otherwise the $\eta^1\text{-CO}_2$ complex ($[\text{Ru}(\text{bpy})_2(\text{CO})(\text{CO}_2)]$), which would be a precursor for formate production, might be stabilized in DMF/water rather than DMA/water. The latter assumption would be led from the report that the $\eta^1\text{-CO}_2$ complex is stabilized by the hydrogen bonding with some solvent molecules.¹⁵ The reason remains unclear, and the research on the CO/formate selectivity is now in progress.

Determination of Oxidation Products of BNAH. It has been known that BNAH can act as not only a one-electron but also a two-electron donor (Supporting Information, Scheme S1). One-electron oxidation of BNAH followed by deprotonation gives a more powerful reductant, BNA^\bullet , than BNAH. In the case of the two-electron oxidation process the BNA^\bullet is further oxidized to give BNA^+ . The one-electron oxidation process gives BNA_2 via the coupling of the BNA^\bullet . Thus, we have identified and quantified the oxidation product of BNAH by using the reversed-phase HPLC on the resulting solution of the photochemical CO_2 reduction. As the oxidation products of BNAH, the stereoisomers of 4,6'- BNA_2 and 4,4'- BNA_2 are observed, while no BNA^+ is detected (Supporting Information, Figure S3). This result is consistent with that observed in the ^{13}C NMR spectra.¹⁴ In the DMA/water solvent system, water molecules are considered to accept the proton from the oxidized BNAH. The total amount of BNA_2 increases, accompanied with decreasing amounts of BNAH, and reaches 0.043 M after photoirradiation for 4 h (Figure 4). The trace of BNA_2 is matched to the total amount of CO and formate, which are quantified within experimental errors by GC. This indicates that the stoichiometry of the reaction is expressed as eq 2.



The decrease of BNAH in Figure 4 does not obey the first-order reaction kinetics, and it gradually becomes slow with passing time. The similar slowdown in the reaction rate has been observed after 2 h in the photocatalytic CO_2 reduction in DMA/water (9:1, v/v), as shown in Figure 2a. The phenomena

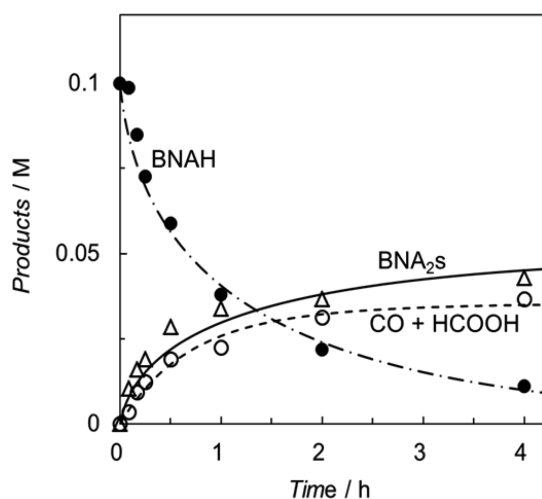


Figure 4. Concentration change of the oxidation and reduction products by the photoirradiation ($\lambda > 400$ nm) of the reaction solution containing $[\text{Ru}(\text{bpy})_2(\text{CO})_2](\text{PF}_6)_2$ (1.0×10^{-4} M), $[\text{Ru}(\text{bpy})_3](\text{PF}_6)_2$ (5.0×10^{-4} M), and BNAH (0.10 M) in the CO_2 -saturated DMA/water (9:1, v/v) solution: BNAH (\bullet), two stereoisomers of 4,6'-BNA₂ and 4,4'-BNA₂ (Δ), and CO+HCOOH (\circ). The simulation curve of [BNAH] was calculated by using the quenching rate constants of BNAH ($k_q = 2.6 \times 10^8 \text{ M}^{-1} \text{ s}^{-1}$) and BNA₂ ($k_q = 1.1 \times 10^9 \text{ M}^{-1} \text{ s}^{-1}$) and the emission lifetime of the excited $[\text{Ru}(\text{bpy})_3]^{2+}$ (0.84 μs). The simulation curve of [BNA₂] was estimated by the equation $[\text{BNA}_2] = 1/2 \times (0.10 - [\text{BNAH}])$.^{3c}

could be explained by the quenching of the excited state of $[\text{Ru}(\text{bpy})_3]^{2+}$ with BNA₂. It has been reported that BNA₂ is a good electron-transfer quencher for the excited $[\text{Ru}(\text{bpy})_3]^{2+}$; however, the BNA₂⁺ and $[\text{Ru}(\text{bpy})_3]^+$ resulting from the quenching efficiently cause the back electron transfer to regenerate BNA₂ and $[\text{Ru}(\text{bpy})_3]^{2+}$.^{3g} To determine the quenching rate constants, we carried out quenching experiments by BNAH and BNA₂ in various DMA/water solvent systems (Supporting Information, Figure S4 and S5). In the DMA/water (9:1, v/v) solution, where the emission lifetime of the excited $[\text{Ru}(\text{bpy})_3]^{2+}$ is 0.84 μs , the quenching rate constant of BNA₂ ($k_q = 1.1 \times 10^9 \text{ M}^{-1} \text{ s}^{-1}$) is 4 times larger than that of BNAH ($k_q = 2.6 \times 10^8 \text{ M}^{-1} \text{ s}^{-1}$). In Figure 4, the concentration changes of BNAH and BNA₂ are simulated based on the quenching rate constants by BNAH and BNA₂. The simulation curves closely match with the experimental plots as well as the slowdown of the reaction rate after 2 h.

We also carried out an experiment in which BNAH is further added to the resulting solution after 3 h of photoirradiation (Supporting Information, Figure S6). The reaction has once slowed down; however, it has recovered after addition of further BNAH. This result strongly suggests that the inactivity of the reaction as observed in Figure 2a does not come from light degradation of $[\text{Ru}(\text{bpy})_2(\text{CO})_2]^{2+}$ or $[\text{Ru}(\text{bpy})_3]^{2+}$ but is due to both the decrease of BNAH and the quenching of the excited $[\text{Ru}(\text{bpy})_3]^{2+}$ ion by the BNA dimer.

Reaction Quantum Yields. We determined the quantum yields for the photocatalytic CO_2 reduction in the DMA/water (9:1, v/v) solution containing $[\text{Ru}(\text{bpy})_2(\text{CO})_2](\text{PF}_6)_2$ (1.0×10^{-4} M), $[\text{Ru}(\text{bpy})_3](\text{PF}_6)_2$ (5.0×10^{-4} M), and BNAH (0.10 M) by using the ferrioxalate actinometer. We used a superhigh-pressure Hg lamp equipped with a cutoff filter (>400 nm). As $[\text{Ru}(\text{bpy})_3]^{2+}$ absorbed the light as the photosensitizer, this combination of lamp and filter results in irradiation light

consisting mainly of 405, 436, and 546 nm wavelengths. For the photochemical CO_2 reduction, the quantum yield Φ can be defined as the molar fraction of the product of CO_2 to the incident photon: the Φ values for CO and formate production are 5.8% and 1.6%, respectively. The total quantum yield corresponding to the photochemical CO_2 reduction is 7.4%. We also utilized a Shimadzu absolute photoreaction quantum yields measurement system QYM-01 to determine the reaction quantum yields. The system monitors the light intensities before and after absorption of the reaction solution and estimates the absorbed light intensity. When irradiated at 460 nm through a monochromator from a 300 W Xe lamp, the reaction quantum yields are determined to be $\Phi_{\text{CO}} = 5.5\%$ and $\Phi_{\text{HCOOH}} = 1.8\%$. Even though the procedure is quite different from the relative method using the chemical actinometer, the quantum yields obtained are almost the same.

The almost-quantitative formation of BNA₂ as the oxidation product of BNAH indicates that one photon induces one electron transfer in the photochemical reaction. Since the CO_2 reduction to CO or formate requires two-electron transfer, the photochemical quantum yield Φ' can be defined by the molar fraction of electron used for the CO_2 reduction to the incident photon, that is, by twice the value of Φ . According to the definition, the quantum yields of the photocatalytic CO_2 reduction in DMA/water (9:1, v/v) are determined to be $\Phi'_{\text{CO}} = 11.6\%$ and $\Phi'_{\text{HCOOH}} = 3.2\%$, and the total yield $\Phi'_{(\text{CO}+\text{HCOOH})}$ is 14.8%. On the other hand, the $\Phi'_{(\text{CO}+\text{HCOOH})}$ in DMF/water (9:1, v/v) is estimated to be 16.5% (literature 17.5%).^{5a} The similar values in DMF/water and DMA/water indicate that DMA can be a good alternative solvent for DMF in this photochemical reaction.

Effects of Water Content on Catalytic Activity. We further examined the effects of water content in the CO_2 -saturated DMA/water solutions on the products of the photochemical reactions (Figure 5a). As observed in the DMF/water solution (Supporting Information, Figure S7a), the total amount of CO and formate is largest at 10 vol % water content and decreases to approximately one-fourth of that when going from 10 to 50 vol % water content. While the largest production of CO is observed at 10 vol % water content, the amounts of formate are similar among the 0, 10, and 20 vol % water content solutions. The smaller production at 0 than at 10 vol % water content indicates that water contributes to the proton source or/and transportation of the protons for the CO_2 reduction.^{5a} The experiments under the Ar-saturated solutions do not afford formate (Figure 5b), in contrast to the reactions in the DMF/water solutions (Supporting Information, Figure S7b).

Increasing the water content, the photocatalytic abilities of CO_2 reduction dramatically decrease. This tendency is also observed in the quenching rate constants of the excited states of $[\text{Ru}(\text{bpy})_3]^{2+}$ quenched by BNAH or BNA₂. The quenching rate constants with BNAH and BNA₂ in the other DMA/water solvent systems are determined from the data shown in Supporting Information, Figures S4 and S5. The Stern–Volmer constants and the quenching rate constants are summarized in Table 1. The quenching fractions (η_q) of the emission from the excited $[\text{Ru}(\text{bpy})_3]^{2+}$ complex with BNAH are also calculated. In all the solvent systems, the excited states of $[\text{Ru}(\text{bpy})_3]^{2+}$ are efficiently quenched; however, the efficiencies decrease by increasing the water contents. In the photocatalytic CO_2 reduction system, the reduced species of $[\text{Ru}(\text{bpy})_3]^{2+}$ is considered to act as an electron relay to the catalyst

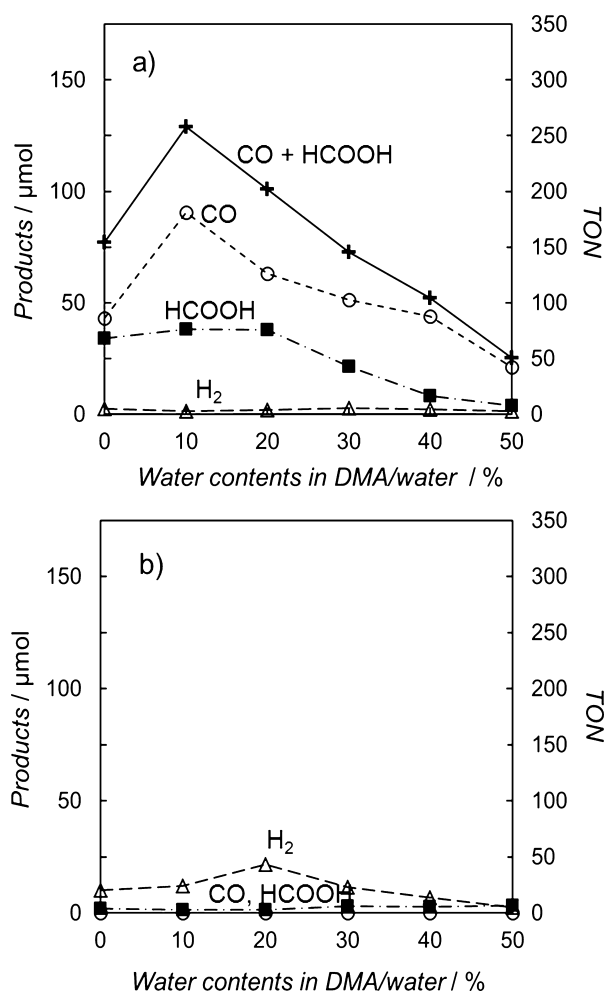


Figure 5. Effects of water content in the (a) CO₂ and (b) Ar-saturated DMA/H₂O solution on the products in the photochemical reaction ($\lambda > 400$ nm, 1 h). [Ru(bpy)₂(CO)₂](PF₆)₂ (1.0×10^{-4} M), [Ru(bpy)₃](PF₆)₂ (5.0×10^{-4} M), and BNAH (0.10 M): CO (○), HCOOH (■), H₂ (Δ), and CO+HCOOH (+).

[Ru(bpy)₂(CO)₂]²⁺. Thus, the decrease of the quenching efficiencies would be a reason why the photocatalytic activities depress at the higher water contents in the DMA/water solution systems.

To know the effects of the water content, we measured the oxidation potentials of BNAH and the reduction potentials of [Ru(bpy)₃]²⁺ with various water contents in DMA/water. As shown in Supporting Information, Table S1, the oxidation potentials of BNAH are independent of the water content,

while the reduction potentials of [Ru(bpy)₃]²⁺ become more negative with increasing water content. These results lead to the decrease of the Gibbs free energy changes ($-\Delta G_{ET}$) in the electron transfer with increasing water content. It indicates that the electron transfer from BNAH to the excited states of ruthenium tris(bipyridine) complex becomes slower with increasing water content in the solution.

CONCLUSION

We demonstrated that DMA can be a good alternative solvent for DMF in the photocatalytic CO₂ reduction, where [Ru(bpy)₂(CO)₂]²⁺, [Ru(bpy)₃]²⁺, and BNAH act as the catalyst, the photosensitizer, and the sacrificial electron donor. The photoreduction of CO₂ proceeded efficiently in the DMA/water (9:1, v/v) solution system, of which the catalytic activities are comparable to those in DMF/water. Furthermore, DMA does not cause the contamination of formate by the hydrolysis, while DMF is partly hydrolyzed to afford formate not during the photoreaction but during the GC analyses. The solvent system using DMA instead of DMF enables us to quantify formate even under harsher analytical conditions such as GC analyses. Even if the amounts of formate yielded by hydrolysis of DMF under Ar are subtracted from the amounts of formate produced in the CO₂ reduction in DMF/water (9:1, v/v), the amounts are larger than those in the CO₂ reduction in DMA/water (9:1, v/v). The reasons for the difference in the CO/formate selectivity between DMF and DMA still remains unclear, and research is now in progress.

ASSOCIATED CONTENT

Supporting Information

Spectra (¹³C NMR) in DMF-d₇/water, photocatalytic CO₂ reduction in several common solvents, scheme for oxidation process of BNAH, Stern–Volmer plots for the quenching by BNAH and 4,6'-BNA₂, time-courses of photocatalytic CO₂ reduction with addition of BNAH, effect of water contents in DMF/water on photocatalytic CO₂ reduction, and the redox potentials of BNAH and [Ru(bpy)₃]²⁺ in DMA/water. This material is available free of charge via the Internet at <http://pubs.acs.org>.

AUTHOR INFORMATION

Corresponding Author

*E-mail: ishida@sci.kitasato-u.ac.jp. Phone: (+81)42-778-9925. Fax: (+81)42-778-9925.

Notes

The authors declare no competing financial interest.

Table 1. Solvent Effects on Quenching Rate Constants of Excited [Ru(bpy)₃]²⁺ by BNAH and 4,6'-BNA₂ in DMA/Water at 298 K

| water content, vol % | τ , μs^a | BNAH | | | 4,6'-BNA ₂ | |
|----------------------|--------------------------|-----------------------------|---|------------------------------|------------------------------|--|
| | | K_{sv} , M ^{-1b} | k_{qt} , M ⁻¹ s ^{-1c} | η_{qt} , % ^d | K_{sv}' , M ^{-1b} | k_{qt}' , M ⁻¹ s ^{-1c} |
| 0 | 0.88 | 394 | 4.5×10^8 | 98 | 1330 | 1.5×10^9 |
| 10 | 0.84 | 217 | 2.6×10^8 | 96 | 915 | 1.1×10^9 |
| 20 | 0.84 | 105 | 1.3×10^8 | 91 | 540 | 6.4×10^8 |
| 30 | 0.82 | 80 | 9.8×10^7 | 89 | 389 | 4.7×10^8 |
| 40 | 0.80 | 44 | 5.5×10^7 | 81 | 242 | 3.0×10^8 |

^aEmission lifetime of [Ru(bpy)₃]²⁺. ^bStern–Volmer constants. ^cQuenching rate constants. ^dQuenching fraction of emission from [Ru(bpy)₃]²⁺ in the presence of 0.1 M BNAH, calculated as $0.1 K_{sv} / (1 + 0.1 K_{sv})$.

ACKNOWLEDGMENTS

We thank Dr. Yusuke Tamaki, Dr. Keita Sekizawa, and Prof. Osamu Ishitani (Tokyo Institute of Technology) for help with capillary electrophoresis analyses, Dr. Yasushi Nakata (Horiba, Ltd.) for emission lifetime experiments, and Mr. Kyohei Fukaya, Mr. Akito Enomoto, and Mr. Makoto Yoshida for experimental supports. This work was supported by the PRESTO Program of JST.

REFERENCES

- (1) (a) Takeda, H.; Ishitani, O. *Coord. Chem. Rev.* **2010**, *254*, 346–354. (b) Tanaka, K. *Chem. Rec.* **2009**, *9*, 169–186. (c) Morris, A. J.; Meyer, G. J.; Fujita, E. *Acc. Chem. Res.* **2009**, *42*, 1983–1994. (d) Marks, T. J.; et al. *Chem. Rev.* **2001**, *101*, 953–996. (e) Fujita, E. *Coord. Chem. Rev.* **1999**, *185–186*, 373–384.
- (2) (a) Suzuki, T. M.; Tanaka, H.; Morikawa, T.; Iwaki, M.; Sato, S.; Saeki, S.; Inoue, M.; Kajino, T.; Motohiro, T. *Chem. Commun.* **2011**, *47*, 8673–8675. (b) Sato, S.; Arai, T.; Morikawa, T.; Uemura, K.; Suzuki, T. M.; Tanaka, H.; Kajino, T. *J. Am. Chem. Soc.* **2011**, *133*, 15240–15243. (c) Sato, S.; Morikawa, T.; Saeki, S.; Kajino, T.; Motohiro, T. *Angew. Chem., Int. Ed.* **2010**, *49*, 5101–5105. (d) Arai, T.; Sato, S.; Uemura, K.; Morikawa, T.; Kajino, T.; Motohiro, T. *Chem. Commun.* **2010**, *46*, 6944–6946.
- (3) (a) Morimoto, T.; Nakajima, T.; Sawa, S.; Nakanishi, R.; Imori, D.; Ishitani, O. *J. Am. Chem. Soc.* **2013**, *135*, 16825–16828. (b) Morimoto, T.; Nishiura, C.; Tanaka, M.; Rohacova, J.; Nakagawa, Y.; Funada, Y.; Koike, K.; Yamamoto, Y.; Shishido, S.; Kojima, T.; Saeki, T.; Ozeki, T.; Ishitani, O. *J. Am. Chem. Soc.* **2013**, *135*, 13266–13269. (c) Voyame, P.; Toghil, K. E.; Méndez, M. A.; Girault, H. H. *Inorg. Chem.* **2013**, *52*, 10949–10957. (d) Tamaki, Y.; Koike, K.; Morimoto, T.; Yamazaki, Y.; Ishitani, O. *Inorg. Chem.* **2013**, *52*, 11902–11909. (e) Tamaki, Y.; Koike, K.; Morimoto, T.; Ishitani, O. *J. Catal.* **2013**, *304*, 22–28. (f) Costentin, C.; Drouet, S.; Robert, M.; Savéant, J.-M. *Science* **2012**, *338*, 90–94. (g) Tamaki, Y.; Morimoto, T.; Koike, K.; Ishitani, O. *Proc. Natl. Acad. Sci. U.S.A.* **2012**, *109*, 15673–15678.
- (4) (a) Lehn, J. M.; Ziessel, R. *J. Organomet. Chem.* **1990**, *382*, 157–173. (b) Hawecker, J.; Lehn, J. M.; Ziessel, R. *J. Chem. Soc., Chem. Commun.* **1985**, 56–58.
- (5) (a) Ishida, H.; Terada, T.; Tanaka, K.; Tanaka, T. *Inorg. Chem.* **1990**, *29*, 905–911. (b) Ishida, H.; Tanaka, K.; Tanaka, T. *Chem. Lett.* **1988**, 339–342. (c) Ishida, H.; Tanaka, K.; Tanaka, T. *Chem. Lett.* **1987**, 1035–1038.
- (6) Paul, A.; Connolly, D.; Schulz, M.; Pryce, M. T.; Vos, J. G. *Inorg. Chem.* **2012**, *51*, 1977–1979.
- (7) (a) Ishida, H.; Fujiki, K.; Ohba, T.; Ohkubo, K.; Tanaka, K.; Terada, T.; Tanaka, T. *J. Chem. Soc., Dalton Trans.* **1990**, 2155–2160. (b) Ishida, H.; Tanaka, H.; Tanaka, K.; Tanaka, T. *J. Chem. Soc., Chem. Commun.* **1987**, 131–132. (c) Ishida, H.; Tanaka, K.; Tanaka, T. *Organometallics* **1987**, *6*, 181–186. (d) Ishida, H.; Tanaka, K.; Tanaka, T. *Chem. Lett.* **1985**, 405–406.
- (8) (a) Agarwal, J.; Fujita, E.; Schaefer, H. F., III; Muckerman, J. T. *J. Am. Chem. Soc.* **2012**, *134*, 5180–5186. (b) Agarwal, J.; Sanders, B. C.; Fujita, E.; Schaefer, H. F., III; Harropcand, T. C.; Muckerman, J. T. *Chem. Commun.* **2012**, *48*, 6797–6799.
- (9) (a) Kelly, J. M.; O'Connell, C. M.; Vos, J. G. *J. Chem. Soc., Dalton Trans.* **1986**, 253–258. (b) Suzuki, K.; Kobayashi, A.; Kaneko, S.; Takehira, K.; Yoshihara, T.; Ishida, H.; Shiina, Y.; Oishi, S.; Tobita, S. *Phys. Chem. Chem. Phys.* **2009**, *11*, 9850–9860.
- (10) (a) Mauzerall, D.; Westheimer, F. H. *J. Am. Chem. Soc.* **1955**, *77*, 2261–2264. (b) Ohnishi, Y.; Kitami, M. *Bull. Chem. Soc. Jpn.* **1979**, *52*, 2674–2677.
- (11) Cicchillo, R. M.; Zhang, H.; Blodgett, J. A. V.; Whitteck, J. T.; Li, G.; Nair, S. K.; van der Donk, W. A.; Metcalf, W. W. *Nature* **2009**, *459*, 871–874.
- (12) (a) Montalti, M.; Credi, A.; Prodi, L.; Gandolfi, M. T. *Handbook of Photochemistry*; 3rd ed.; CRC Press: Boca Raton, FL, 2006.

(b) Hatchard, C. G.; Parker, C. A. *Proc. R. Soc. London, Ser. A* **1956**, *235*, 518–536.

(13) Kankaanperä, A.; Scharlin, P.; Kuusisto, I.; Kallio, R.; Bernoulli, E. *J. Chem. Soc., Perkin Trans. 2* **1999**, 169–174.

(14) Moracci, F. M.; Liberatore, F.; Carelli, V.; Arnone, A.; Carelli, I.; Cardinali, M. E. *J. Org. Chem.* **1978**, *43*, 3420–3422.

(15) (a) Tanaka, H.; Tzeng, B.-C.; Nagao, H.; Peng, S.-M.; Tanaka, K. *Inorg. Chem.* **1993**, *32*, 1508–1512. (b) Tanaka, H.; Nagao, H.; Peng, S.-M.; Tanaka, K. *Organometallics* **1992**, *11*, 1450–1451.